DOI: 10.1002/ejoc.201000184

Theoretical Study on Hetero-Diels–Alder Reaction of Butadiene with Benzaldehyde Catalyzed by Chiral In^{III} Complexes

Xiuli Cao,[a] Song Qin,[a] Zhishan Su,[a] Huaqing Yang,[a] Changwei Hu,*[a] and Xiaoming Feng*[a]

Keywords: Reaction mechanisms / Cycloaddition / Indium / Density functional calculations

The mechanism of the hetero-Diels–Alder reaction of butadiene with benzaldehyde catalyzed by chiral *N*,*N*′-dioxide/$In(OTf)_3$ complexes was studied theoretically by using density functional theory (DFT) and model system. The computational results indicate that the catalyzed reaction proceeded through a concerted mechanism via a highly zwitterionic transition state. The lowest energy barrier was 11.8 kJ mol^{-1}, which is 63.0 kJ mol^{-1} lower than that of the uncatalyzed reaction. The results indicate that the *endo* approach is advantageous over the *exo* approach, because *exo* transitions states suffer from more steric hindrance than the *endo* transitions states as a result of interactions among the substrates, the trifluoromethanesulfonic group and the R^4 groups of the ligand. The (*S*) configuration was observed predominantly over the (*R*) form, because there is no distinguishable repulsion between butadiene and the *exo* amino side or the *endo* amino side of the ligand. Besides, the interactions between the terminal hydrogen atoms of butadiene and the oxygen atoms of the trifluoromethanesulfonic group make the structure more stable. Thus, the experimental results were explained well by calculation of the chiral *N*,*N*′-dioxide/In-$(OTf)_3$ complex catalyzed hetero-Diels–Alder reaction at the molecular level.

Introduction

Hetero-Diels–Alder (HDA) reaction between 1,3-dienes and carbonyl compounds is one of the most useful methods to prepare optically active six-membered heterocyclic compounds.[1,2] These compounds are extensively applied in many bioactive natural products and important pharmaceuticals.[3] Many chiral Lewis acids based on metal complexes, such as the complexes based on titanium,[4] boron,[5] chromium,[6] magnesium,[7] aluminum,[8] and dirhodium,[9] have been successfully designed as catalysts for this type of reaction. Very recently, indium complexes[10] as effective Lewis acid catalysts have been developed for carbon–carbon bond-forming reactions and other synthetic processes.[11] The Feng group[12] synthesized a series of novel and efficient chiral catalysts based on *N*,*N*′-dioxide/In-$(OTf)_3$ complexes and used them in asymmetric HDA reactions. Remarkable improvements were obtained with an extremely broad range of substrates, and this reaction produced highly substituted chiral pyranones in good yields with up to 99%*ee* (Scheme 1).

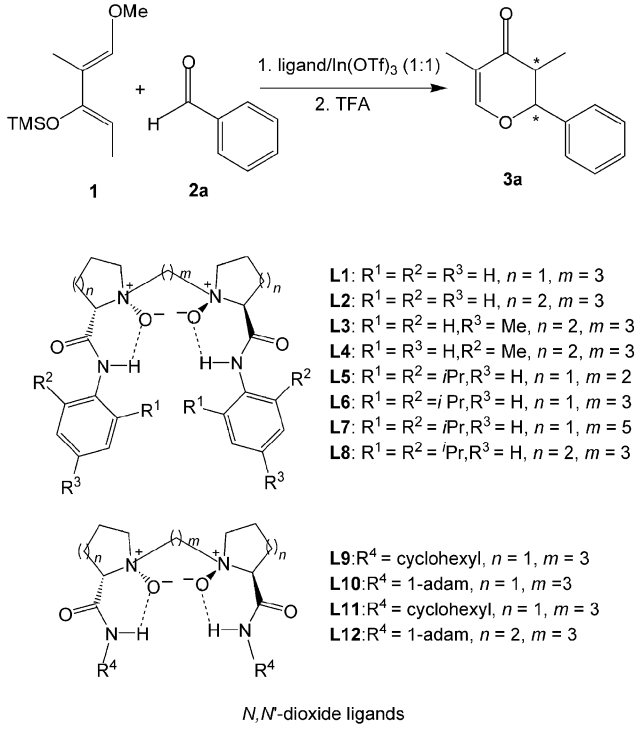

Scheme 1. The asymmetric hetero-Diels–Alder reaction of benzaldehyde with diene **1** catalyzed by *N*,*N*′-dioxide/$In(OTf)_3$ complexes.

Though accumulated theoretical reports are available in this area,[13] apart from the numerous effort devoted to the synthetic aspects of asymmetric HDA reactions, the mecha-

[a] Key Laboratory of Green Chemistry and Technology, Ministry of Education, College of Chemistry, Sichuan University, Chengdu, Sichuan, 610064, P. R. China
Fax: +86-28-85411105
E-mail: chwehu@mail.sc.cninfo.net
gchem@scu.edu.cn

Supporting information for this article is available on the WWW under http://dx.doi.org/10.1002/ejoc.201000184.

nism of the HDA reaction is still attractive for theoretical investigations. The mechanism of the HDA reaction could generally fall into two different categories: Mukaiyama aldol reaction pathway versus traditional Diels–Alder cycloaddition pathway (Scheme 2).[1a,13d] Houk and coworkers[5a,14] calculated the HDA reaction between formaldehyde and butadiene. They found that the uncatalyzed reaction might proceed along a concerted pathway via an asymmetric transition structure. When Lewis acid BH_3 (the catalyst) coordinated to the oxygen atom of formaldehyde, the activation energy of the reaction decreased drastically and the asynchronicity increased in the transition structure. Later, the Jørgensen group[15] studied the reaction of benzaldehyde with Danishefsky's diene catalyzed by various aluminum complexes by using AM1 and ab initio methods. Their results indicated that the concerted reaction occurred most likely through the Diels–Alder cycloaddition mechanism without any catalysts, although Mukaiyama aldol pathways were found when the reactions were catalyzed by $(MeO)_2AlMe$ and (*S*)-BINOL/AlMe. the Domingo group[16] investigated the effect of hydrogen bonding involving molecules on the model HDA reaction of the butadiene derivative with acetone by using DFT calculations at the B3LYP/6-31+G(d) level. Their results suggested that in the gas phase, the formation of hydrogen bonds decreased the activation energies of the reaction. The mechanism was sensitive to solvent effects, for it could be changed from a concerted process without solvent to a two-step mechanism in the presence of chloroform. Zhang et al.[17] reported computational studies on the catalysis and enantioselectivities of the HDA reaction of benzaldehyde with Danishefsky's diene catalyzed by α,α,α′,α′-tetraaryl-1,3-dioxolane-4,5-dimethanol (TADDOL) derivatives by using the ONIOM (B3LYP/6-31G*:PM3) method. The results indicated that this reaction proceeded through a concerted mechanism via an asynchronous and zwitterionic transition structure, and benzaldehyde was activated by forming an intermolecular hydrogen bond with TADDOL. Moreover, the bulky aryl substituents in the TADDOL catalyst effectively controlled the enantioselectivity of this reaction. Yamada and coworkers[18] carried out a detailed theoretical analysis on the HDA reaction catalyzed by cobalt complexes by using the B3LYP/[6-31G*:LANL2DZ] method. The results revealed that the activation energy decreased due to the cationic character of the cobalt atom. Formaldehyde coordinated axially to the cobalt center and increased the Lewis acidity of the catalyst, and therefore, the enantioselectivity for the overall reaction was improved. Recently, the Chaquin group[19] investigated the influence of the configuration of the double bond on the regio- and *endo*-selectivity in Diels–Alder reactions. The origin of the selectivities was attributed to the balance between steric hindrance and electrostatic interaction.

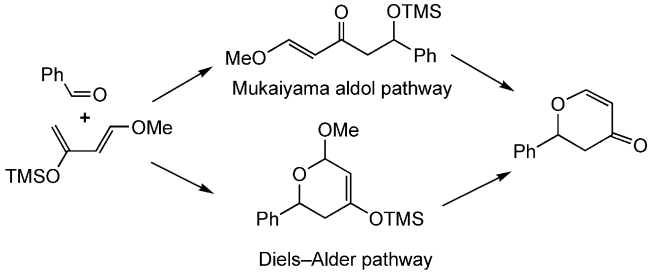

Scheme 2. The two different reaction pathways for the hetero-Diels–Alder reaction.

To our best knowledge, however, there is no detailed theoretical investigation based on quantum chemistry that is available in the literature that is aimed at the mechanism and stereochemistry of HDA reactions catalyzed by chiral *N*,*N*′-dioxide/$In(OTf)_3$ complexes. For the sake of gaining a better understanding of this reaction and providing useful clues to the asymmetric synthesis, the present theoretical simulation on the mechanism and stereochemical nature of the catalytic enantioselective hetero-Diels–Alder reaction of benzaldehyde with Danishefsky's diene catalyzed by chiral *N*,*N*′-dioxide/$In(OTf)_3$ complexes was carried out. This work is expected to be useful for the design of new catalysts based on chiral metal–*N*,*N*′-dioxide ligand complexes.

Models and Computational Details

All calculations were performed within the density functional theory in the Gaussian 03 programs.[20] The unrestricted Becke three-parameter hybrid exchange functional combined with the Lee–Yang–Parr correlation functional (B3LYP)[21] was used for geometry optimizations and vibrational calculations. The basis sets were LANL2DZ[22] with the Hay and Wadt's effective core potential (ECP) for the indium atom, and the 6-31G(d,p)[23] basis set was used for all other elements. Each geometry was analyzed by harmonic vibrational frequencies obtained at the same level and characterized as a minimum (no imaginary frequency) or a transition state (one imaginary frequency). Considering the effect of the solvent, single-point B3LYP (PCM,[24] THF)/[6-311++G(d,p):LANL2DZ] calculations were performed on the optimized structures. The relative energies of the optimized structures were corrected by zero-point energy (ZPE). Basis-set superposition error (BSSE) corrections were applied. Unless otherwise specified, the discussed energies are relative Gibbs free energies in THF without ZPE correction. The electronic structures of stationary points were analyzed by the Natural Bond Orbital (NBO) method[25] and the charge transfer (CT) at the transitions states was analyzed with the NBO method.[26] Because the global electrophilicity index[27] ω measured the stabilization energy when the system acquires an additional electronic charge from the environment, the global electrophilicity parameter was considered, which had the expression as $\omega = \mu^2/2\eta$ (the electronic chemical potential μ and the chemical hardness η).

In the most related literature, the electrospray ionization mass spectrometry (ESI-HRMS) data obtained by the group of Feng suggested that the *N*,*N*′-dioxide ligand might lose the two hydrogen atoms of the amide moieties, ac-

companied by the release of two HOTf molecules, and therefore, the catalyst in the L-In(OTf) form might be generated.[12] On this basis, it is assumed that the chiral ligand could coordinate to the indium center to form a *N*,*N*′-dioxide–indium catalyst by two N–In bonds and two O–In bonds. Considering the rigidity and C_2 symmetry of the ligand, two geometries were designed as the initial structures for conformational search (In-Lm-α and In-Lm-β, Scheme 3). In In-Lm-α, N^1–O^1, N^3, and N^4 occupy the equatorial position, whereas N^2–O^2 and the OTf group occupy the axial positions in the trigonal bipyramid conformation. In In-Lm-β, N^3 and the OTf group exchange their positions in the trigonal bipyramid conformation. Through geometry optimization, In-Lm-α was identified as the stable structure. However, the calculations failed to locate the In-Lm-β conformation as an energy minimum on the potential energy surface, as the geometry optimization for it always converged to In-Lm-α. Therefore, In-Lm-α was selected as the conformation of the catalyst in our models.

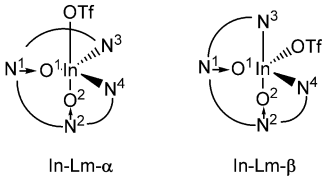

Scheme 3. Initial structures of the catalyst for conformational search.

Here, two models were used in the following investigations to probe the mechanism and stereochemistry of the catalytic reaction between benzaldehyde and Danishefsky's diene catalyzed by chiral *N*,*N*′-dioxide/In(OTf)$_3$ complexes. To reduce the computational cost and obtain reliable results, in model I, Danishefsky's diene was replaced by a simple butadiene, and benzaldehyde was replaced by formaldehyde. The bulky structural moiety R^4 of the chiral ligands was replaced by a methyl group (Scheme 4).

The second model (model II) was used to examine the stereochemistry of the reaction at the molecular level. In model II, a prochiral substrate benzaldehyde was used to replace the formaldehyde in model I to extend our theoretical investigation on the stereoselectivity of the HDA reaction (Scheme 4).

Results and Discussion

The predicted mechanism is shown in Figure 1. Relative energies for various species along the predicted reaction pathways in model I are listed in Table 1. Figure 2 depicts the reaction energy profiles for the reaction of formaldehyde and butadiene catalyzed by chiral *N*,*N*′-dioxide/In(OTf)$_3$ complexes in tetrahydrofuran (THF), and Figure 3 depicts the optimized geometries of the stationary points.

Uncatalyzed Reaction of Butadiene and Formaldehyde

Previously, the Houk group reported calculations on the uncatalyzed reaction of butadiene with formaldehyde and proposed that the reaction involved a concerted mechanism.[14] In this section, we performed similar calculations to evaluate the background reaction of formaldehyde and 1,3-butadiene at our level (B3LYP/6-31G*). Our present DFT calculations on this system indicate that the uncatalyzed reaction proceeds through a concerted pathway, and no zwitterionic intermediate or transition state (TS) corresponding to the Mukaiyama aldol-type pathway could be located. For the TS, the C–C and C–O bond lengths are 1.996 and 2.144 Å, respectively. The energy barrier for this transition state leading to dihydropyran was calculated to be 88.8 kJ mol^{-1} in the gas phase, and it decreased to 74.8 kJ mol^{-1} in THF. The vibration mode of its unique imaginary frequency suggests that the reaction corresponds to a concerted Diels–Alder cycloaddition mechanism. These data are consistent with the calculation results reported previously by the Houk group.[14]

Formation of Catalyst–Formaldehyde Complexes

In the presence of the catalyst, the coordination of the oxygen atom of formaldehyde to the indium atom may take place. This process leads to the formation of two diastereotopic catalyst–substrate complexes (COM-a and COM-b, Figure 1). The electrophilicity of COM-a (ω = 7.57 eV) and COM-b (ω = 7.46 eV) is much higher than that of In-Lm (ω = 2.67 eV), which infers that COM-a and COM-b possess remarkably greater electrophilicity than In-

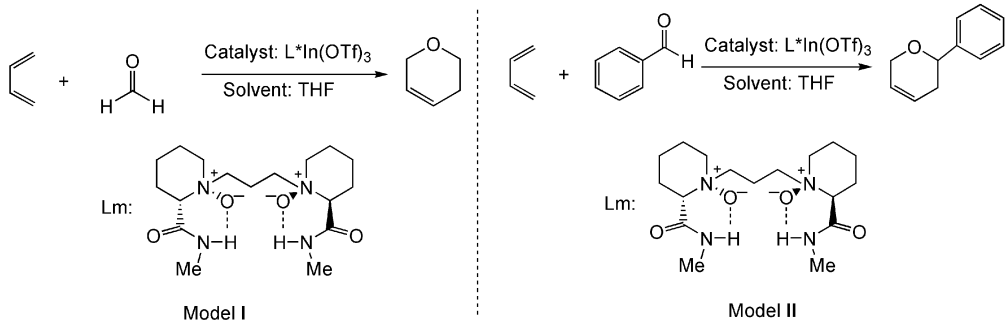

Scheme 4. Model systems for hetero-Diels–Alder reaction.

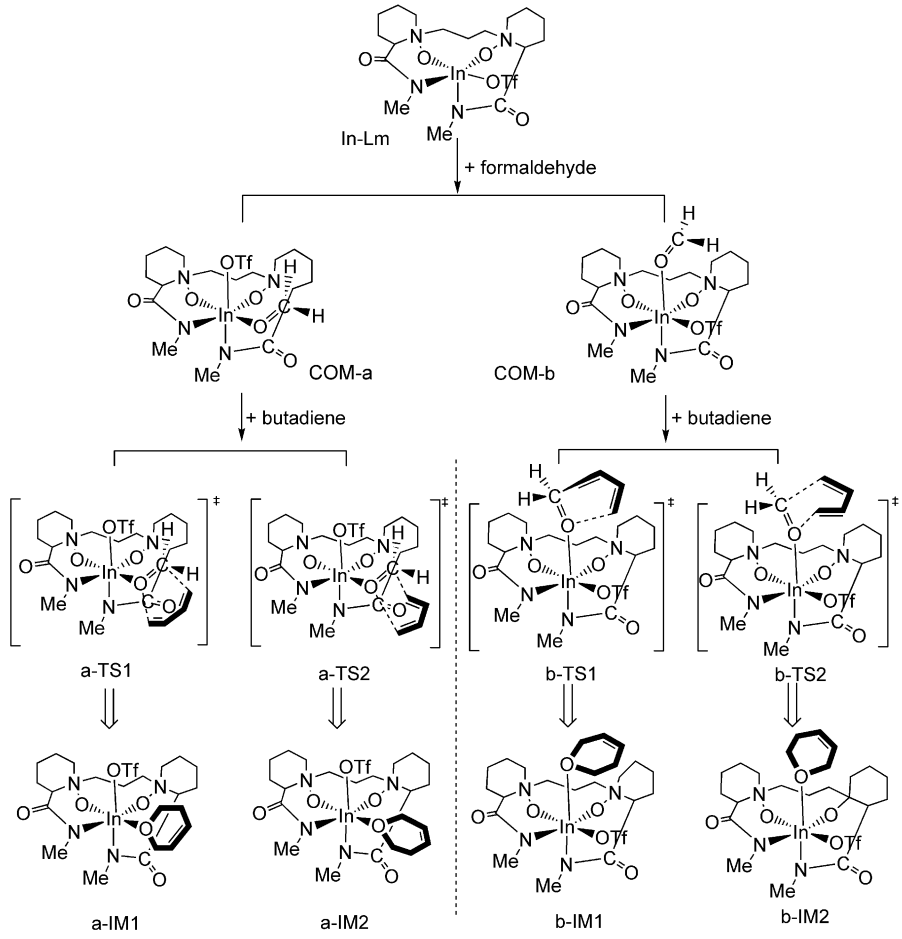

Figure 1. The predicted hetero-Diels–Alder reaction mechanism over the model catalyst In-Lm.

Table 1. Relative energies in the gas phase at the B3LYP/[6-31G(d):LANL2DZ] level and in THF at the B3LYP/[6-311++G(d,p):LANL2DZ] level for all species along the predicted reaction pathways in model I and charge transfer at the TSs.

Species	ΔE [kJ mol^{-1}]	ΔE (int,BSSE) [kJ mol^{-1}]	ΔG [kJ mol^{-1}]	ΔG (int,BSSE) [kJ mol^{-1}]	CT [e]
Reactants[a]	23.2	4.1	–12.1	–13.0	–
COM-a + diene	0.0	0.0	0.0	0	–
a-TS1	62.2	34.9	36.9	11.8	0.318
a-IM1	–104.8	–102.1	–124.6	–121.8	–
a-TS2	61.4	34.1	38.6	13.4	0.389
a-IM2	–97.7	–61.8	–120.3	–84.5	–
COM-b + diene	12.5	13.4	–0.7	0.09	–
b-TS1	83.1	55.8	52.9	27.8	0.387
b-IM1	–74.1	–81.1	–99.3	–104.5	–
b-TS2	87.9	60.6	54.7	29.6	0.406
b-IM2	–82.9	–81.0	–109.4	–106.5	–
Products[b]	–78.6	–105.9	–100.8	–125.9	–

[a] Reactants: In-Lm + diene + formaldehyde. [b] Products: In-Lm + dihydropyran.

Lm and then could serve as an electrophile in cycloaddition with butadiene. The optimized geometries illustrate that there exists a hexacoordinated indium center in each complex. The In–O_f (oxygen atom of formaldehyde) and In–O_t (oxygen atom of trifluoromethanesulfonic group) bond lengths are 2.310 and 2.302 Å in COM-a and 2.687 and 2.135 Å in COM-b, respectively. Because COM-a is comparable to its analogue COM-b in relative energies, these two complexes might co-exist in the system and the subsequent reaction might alternatively occur from each of them.

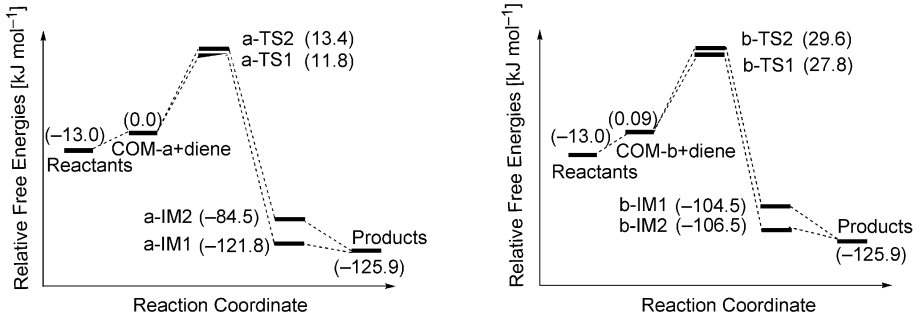

Figure 2. Energy profiles for the hetero-Diels–Alder reaction of formaldehyde and butadiene in THF catalyzed by chiral indium(III) complexes along path-a1, path-a2, path-b1, and path-b2.

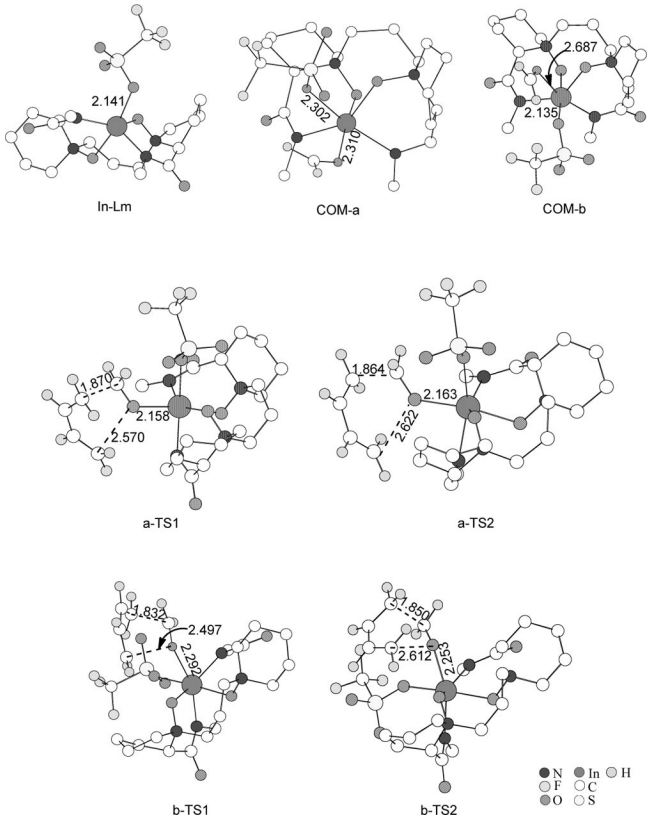

Figure 3. Optimized geometries of the stationary points for model I. Selected distances are given in Å and some hydrogen atoms are omitted for clarity.

Addition of Butadiene to COM-a and COM-b

For each formaldehyde–catalyst complex (COM-a or COM-b), 1,3-butadiene can alternatively approach formaldehyde from two sides (the *endo* amide side and the *exo* amide side, Figure 1). As a consequence, four different reaction pathways may result (path-a1, path-a2 and path-b1, path-b2).

As shown in Figure 1, along reaction path-a1, an external butadiene initially gets close to the COM-a skeleton from the *endo* amino side and then attacks the formaldehyde in COM-a via transition state a-TS1, which leads to the formation of product complex a-IM1. Then, the release of dihydropyran takes place with the recovery of model catalyst In-Lm. For a-TS1, the carbon atoms of formaldehyde interact strongly with one ending carbon atom of butadiene, whereas the oxygen atom of formaldehyde interacts strongly with the other ending carbon atom of butadiene. The reactants lie –13.0 kJ mol^{-1} below the electrostatic complex (COM-a and butadiene) in relative Gibbs energies in THF. The C–C and C–O bond lengths in a-TS1 are calculated to be 1.870 and 2.570 Å, respectively. NBO analysis shows that transition state a-TS1 has a partial positive charge of +0.38 on butadiene, a negative charge of –0.61 on the formaldehyde oxygen atom, and a negative charge of –0.10 on indium catalyst In-Lm. Hence, the coordination of the carbonyl oxygen atom to indium makes the carbonyl group accept the negative charge, and the In–O_f bond length in a-TS1 decreases by 0.152 Å from 2.310 Å in COM-a, indicating a tighter complexation in a-TS1. According to the overall geometry of the transition state, it can be concluded that the transition state along path-a1 of the catalyzed reaction may be of asynchronicity in general. The calculation suggests that a-TS1 is 11.8 kJ mol^{-1} higher than butadiene and COM-a in relative Gibbs energy.

On the other hand, as shown in Figure 1, there exists a parallel reaction pathway marked as path-a2 for COM-a. Along this reaction pathway, an external butadiene initially approaches to the COM-a skeleton from the *exo* amide side and then attacks formaldehyde on COM-a via transition state a-TS2. The following reaction steps are predicted similar to the reaction along pathway a1. The transition state a-TS2 lies 13.4 kJ mol^{-1} higher than that of the electrostatic complex (COM-a and butadiene) on potential energy surface (PES). The carbon atom and the oxygen atom of formaldehyde also have strong interactions with the ending carbon atoms of butadiene correspondingly. For transition-state a-TS2, the C–C and C–O bond lengths are calculated to be 1.864 and 2.622 Å, respectively. It owns a partial positive charge of +0.39 on butadiene, a negative charge of –0.58 on the formaldehyde oxygen atom, and a negative charge of –0.10 on indium catalyst In-Lm.

As mentioned above, the reaction can also occur along path-b1 and path-b2. The mechanisms of path-b1 and path-b2 are fairly similar with those of path-a1 and path-a2, and

the energy barriers of transition states b-TS1 and b-TS2 (27.8 and 29.6 kJ mol^{-1}, respectively) were obviously larger than those of path-a1 and path-a2. The dissociation of dihydropyran is exothermic in all the pathways, which might be due to the solvent effect in the reaction. To make a brief expression, we do not discuss them in detail.

These four pathways (path-a1, path-a2, path-b1 and path-b2) share the similar concerted reaction mechanism with asynchronous transition states. Path-a1 is kinetically more favorable than the other three pathways (path-a2, path-b1, and path-b2). Compared with the uncatalyzed reaction, path-a1 is favored in 63.0 kJ mol^{-1} of energy barrier. These results demonstrate that the *N*,*N*′-dioxide indium complex decreases the energy barrier significantly and exhibits an obvious catalytic performance in HDA reaction.

To probe the electronic properties of the reaction system, charge transfer (CT) analysis of the corresponding TSs was carried out (as shown in Table 1). For the uncatalyzed reaction, the CT value of the TS is 0.188 e. For the catalyzed reaction, the natural charges at the TSs are shared between the butadiene and the dienophiles of COM-a or COM-b. CT value of TSs varies in the range from 0.381 to 0.406 e, which indicates that these structures may be of zwitterionic character, and the reaction processes present an asynchrony electron movement. It can be summarized that the coordination of the carbonyl oxygen atom of the formaldehyde to Lewis acid indium catalyst modifies the electronic properties and then increases the polar characters of the system, leading to the decrease in the energy barriers.

In terms of ligand, the Jørgensen group[15] employed the chiral 1,1′-binaphthol (BINOL) ligand and the Yamada group[19] adopted the salen ligand. They also performed theoretical studies on HDA reactions catalyzed by metal (aluminum and cobalt, respectively) complexes. The Gibbs energy barrier of our model reaction system is 11.8 kJ mol^{-1} (36.9 kJ mol^{-1} without BSSE correction), which is lower than that reported by the Jørgensen (54.4 kJ mol^{-1}) and Yamada (55.2 kJ mol^{-1}) groups, implying that chiral *N*,*N*′-dioxide indium complex shows excellent catalytic performance. Our theoretical investigation of energy barriers and the CT values on model I verified the report by Feng that the *N*,*N*′-dioxide indium complex is an effective catalyst.

Stereoselectivity of In^{III}-Catalyzed HDA Reactions

The stereoselectivity of the HDA reaction is so attractive that great endeavors have been devoted to this area in recent years. High yields (above 92% yield) and excellent *ee* values (99%*ee*) were obtained by the group of Feng,[12] which indicated that the chiral *N*,*N*′-dioxide/In(OTf)$_3$ catalyst showed not only good catalytic effect but also excellent stereoselectivity for the HDA reaction. Although our above investigation successfully explained the catalytic effect of the *N*,*N*′-dioxide/In(OTf)$_3$ catalyst for the HDA reaction, it was not sufficient to interpret the stereoselectivity of the chiral *N*,*N*′-dioxide/In(OTf)$_3$-catalyzed reaction. In this section, model II (Scheme 4) is used to extend our theoretical investigation to the stereoselectivity of the HDA reaction.

Starting from COM-a and COM-b, there exist four diastereotopic catalyst–benzaldehyde complexes (C1 and C2; C3 and C4). As shown in Figure 4, the coordination of trifluoromethanesulfonic group orientates toward the six-membered rings of the ligand in C1, whereas benzaldehyde orientates toward the six-membered rings of the ligand in C2. As compared to C1 and C2, phenyl groups of the benzaldehyde in C3 and C4 are on the opposite side, respectively. From each catalyst–benzaldehyde complex, the reaction could occur via four instinct TSs (*endo*-TS-*Si*/*endo*-TS-*Re*, *exo*-TS-*Si*/*exo*-TS-*Re*). Thus, 16 TSs could result in the entire set of calculated pathways, marked as *endo*-TS-*Si*-a/*endo*-TS-*Re*-a, *exo*-TS-*Si*-a/*exo*-TS-*Re*-a and *endo*-TS-*Si*-b/*endo*-TS-*Re*-b, *exo*-TS-*Si*-b/*exo*-TS-*Re*-b, and *endo*-TS-*Si*-a1/*endo*-TS-*Re*-a1, *exo*-TS-*Si*-a1/*exo*-TS-*Re*-a1 and *endo*-TS-*Si*-b1/*endo*-TS-*Re*-b1, *exo*-TS-*Si*-b1/*exo*-TS-*Re*-b1, respectively. The prefixes *exo*/*endo* present the *exo*/*endo* approaches of the dienophile to the butadiene and the infixes *Re*/*Si* present the direction of the attack of butadiene to the *Re* or *Si* face of the In-Lm activated benzaldehyde.

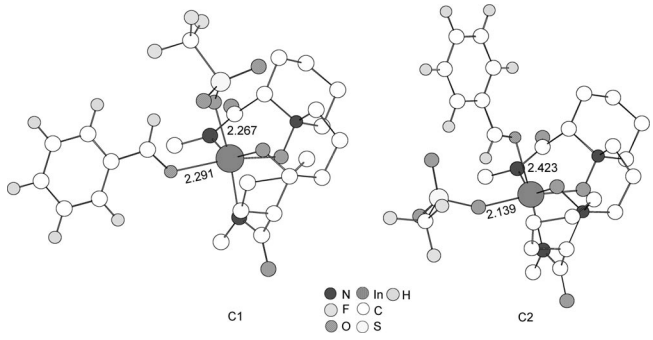

Figure 4. Two different diastereotopic catalyst–benzaldehyde complexes (C1 and C2) in the reaction of benzaldehyde and butadiene catalyzed by In-Lm. Selected distances are given in Å and some hydrogen atoms are omitted for clarity.

Figure 4 presents two different diastereotopic catalyst–benzaldehyde complexes C1 and C2. Figure 5 presents the selected transition states (*exo* and *endo* approach) of the HDA reaction of benzaldehyde with butadiene catalyzed by In-Lm. The relative Gibbs energy barriers and CT analysis of the 16 TSs are listed in Table 2.

In model II, the CT at TSs ranges from 0.393 to 0.499 e, except for the values of *endo*-TS-*Re*-b1 (0.263 e) and *exo*-TS-*Re*-b1 (0.255 e). Thus, the polar character of model II is greater than that of model I. The extent of asynchronous bond formation is larger than that of model I. It may be explained by the fact that the electron-releasing group (-Ph) enhances the electron transfer between the diene and the dienophile of C1 or C2.

As shown in Table 2, except for *exo*-TS-*Si*-b1, the energy barriers of *endo* TSs are lower than those of the *exo* TSs. Along the reaction pathway from C1, the energy barriers of *endo*-TS-*Si*-a and *endo*-TS-*Re*-a are 90.8 and 105.4 kJ mol^{-1}, respectively. In contrast, the energy barriers of *exo*-TS-*Si*-a and *exo*-TS-*Re*-a are 110.8 and

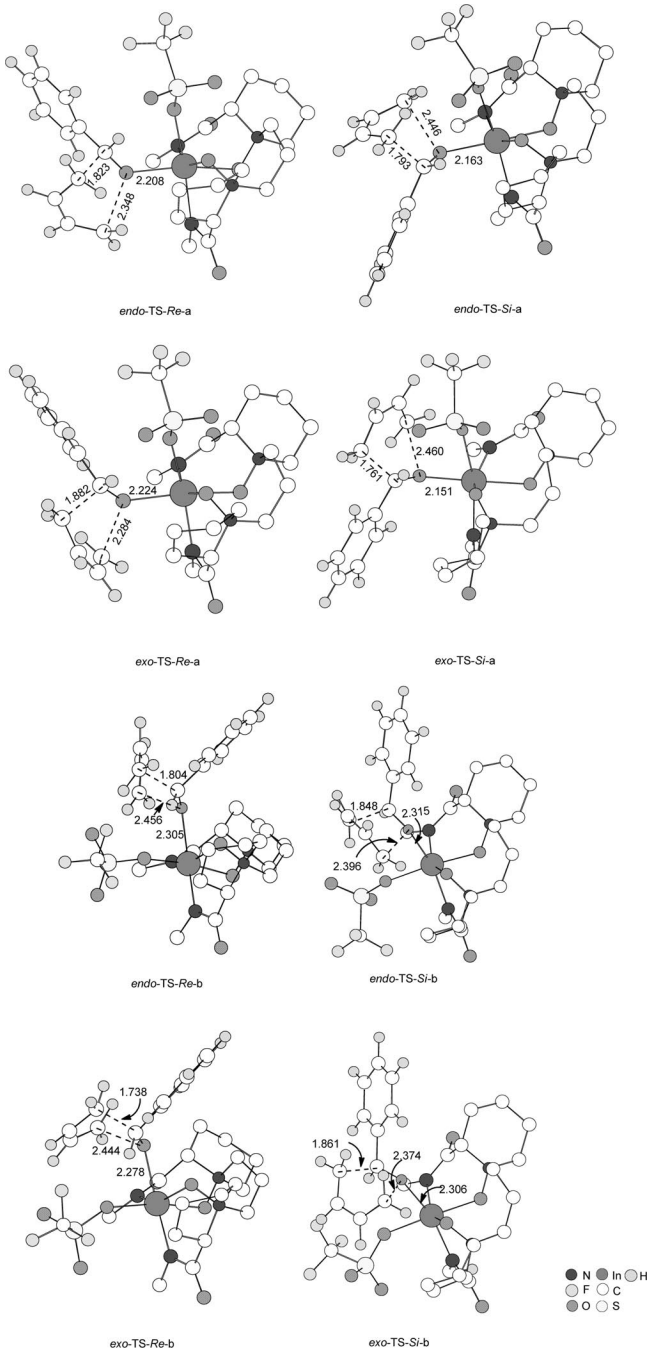

Figure 5. The selected transition states in the reaction (*endo* and *exo* approaches) of benzaldehyde and butadiene catalyzed by In-Lm. Selected distances are given in Å and some hydrogen atoms are omitted for clarity.

113.0 kJ mol^{-1}, respectively. On the other hand, along the reaction channel from C2, the energy barrier of *endo*-TS-*Si*-b is 106.0 kJ mol^{-1} and that of *exo*-TS-*Si*-b is 118.0 kJ mol^{-1}. It is obvious that *exo* TSs suffer more steric hindrance than *endo* TSs, which originates from the mutual repulsion among the substrates, the trifluoromethanesulfonic group, and the R^4 groups of the ligand. These results enrich the previous theoretical results,[4,18,28] in which *endo* approach is more favorable than *exo* approach.

Table 2. Relative energies in THF at the B3LYP/[6-311++G(d,p):LANL2DZ] level for the selected transition states (*exo* and *endo* approaches) of the HDA reaction of benzaldehyde with butadiene catalyzed by In-Lm.

Species	ΔG [kJ mol^{-1}]	τ [%][a]	Config.	CT [e]
C1 + diene	0.0	–	–	–
endo-TS-*Si*-a	90.8	96.09	*S*	0.492
endo-TS-*Re*-a	105.4	0.27	*R*	0.413
exo-TS-*Si*-a	110.8	0.03	*S*	0.490
exo-TS-*Re*-a	113.0	0.01	*R*	0.393
C2 + diene	10.6	–	–	–
endo-TS-*Si*-b	106.0	0.21	*S*	0.420
endo-TS-*Re*-b	103.3	0.62	*R*	0.453
exo-TS-*Si*-b	118.0	–	*S*	0.421
exo-TS-*Re*-b	113.3	0.01	*R*	0.499
C3 + diene	5.6	–	–	–
endo-TS-*Si*-a1	115.0	–	*S*	0.410
endo-TS-*Re*-a1	99.9	2.44	*R*	0.430
exo-TS-*Si*-a1	147.2	–	*S*	0.378
exo-TS-*Re*-a1	104.9	0.32	*R*	0.434
C4 + diene	44.0	–	–	–
endo-TS-*Si*-b1	141.5	–	*S*	0.426
endo-TS-*Re*-b1	140.9	–	*R*	0.263
exo-TS-*Si*-b1	124.1	–	*S*	0.426
exo-TS-*Re*-b1	142.8	–	*R*	0.255

[a] τ: Occupied probability based on Boltzmann distribution, $\tau = N_i^*/N = [g_i\exp(-\varepsilon_i/kT)]/[\sum g_i\exp(-\varepsilon_i/kT)]$ (T = 298.15 K). *ee* = $(\sum\tau^S - \sum\tau^R)/\sum(\tau^R + \tau^S)$ = 93%.

As shown in Table 2, for the competing TSs (*endo*-TS-*Si*-a and *endo*-TS-*Re*-a), the energy barrier of *endo*-TS-*Si*-a is calculated to be 14.6 kJ mol^{-1} lower than the other. Considering the entire set of calculated pathways, the energy differences from B3LYP/[6-311++G(d,p):LANL2DZ] single-point calculations predict that the selectivity for the formation of the corresponding (*S*) product should be >96% (corresponding to 93% *ee*) on the basis of the Boltzmann distribution in Table 2, which is in agreement with the experimental value (99% *ee*). The above results indicate that the (*S*) configuration is preferred to the (*R*) configuration. This might be attributed to two main reasons: (i) For the structure of *endo*-TS-*Si*-a, there is no distinguishable repulsion between the butadiene and the *exo* amino side or the *endo* amino side of the chiral ligand. The interactions between the terminal hydrogen atoms of butadiene and the oxygen atoms of the trifluoromethanesulfonic group (2.300 and 2.451 Å, respectively) make the structure *endo*-TS-*Si*-a more stable. (ii) In *endo*-TS-*Re*-a, there exists larger repulsion between butadiene and the six-membered ring of the *exo* amino side of the chiral ligand and no stabilization interaction is presented between butadiene and the trifluoromethanesulfonic group (Figure 6). Therefore, with the induction of In-O catalysis, the (*S*) configuration might be the predominant product in the reaction. The above simulation at the molecule level successfully explains the observation in the experiments of Feng.

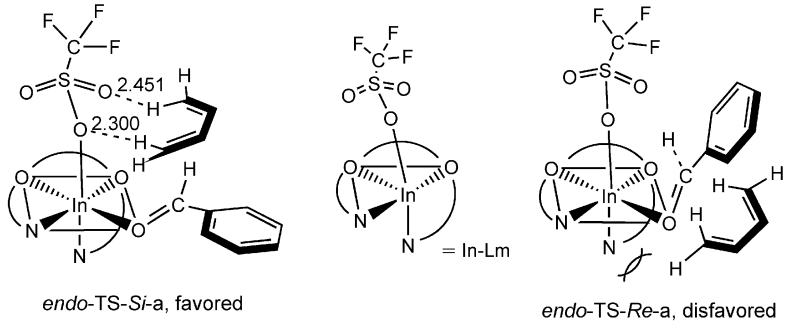

Figure 6. Comparison of the competing TSs (*endo*-TS-*Si*-a and *endo*-TS-*Re*-a). Selected distances are given in Å.

According to the above theoretical results, a further reasonable deduction can be drawn. When a ligand with larger substituents is used, the difference in the steric hindrance between the substrate and the ligand increases, which then enhances the stereoselectivity. This assumption is in accord with the experimental fact that the introduction of sterically bulky R^4 groups of ligand L8 remarkably improves the stereochemistry of the asymmetric HDA reaction.[12]

Conclusions

The mechanism of the HDA reaction of butadiene with benzaldehyde catalyzed by chiral *N*,*N*′-dioxide/In(OTf)$_3$ complexes was studied theoretically by using DFT and model systems. The major conclusions can be summarized as the following: (1) HDA reactions catalyzed by *N*,*N*′-dioxide/In(OTf)$_3$ complexes proceeded through a concerted mechanism via an asynchronous and zwitterionic transition structure with a much lower energy barrier compared to the uncatalyzed reaction. (2) There were obvious preferences for the *endo* approach over the *exo* approach when the diene attacks the benzaldehyde, because the *exo* TSs suffer more steric hindrance than *endo* TSs, which originates from the mutual repulsion among the substrates, the trifluoromethanesulfonic group, and the R^4 groups of the ligand. (3) The (*S*) configuration is preferred over the (*R*) configuration, because there is no distinguishable repulsion between the diene and the *exo* amino side or the *endo* amino side of the chiral ligand. Moreover, the interactions between the terminal hydrogen atoms of butadiene and the oxygen atoms of trifluoromethanesulfonic group make the structure more stable.

Supporting Information (see footnote on the first page of this article): Computational methods for the model systems, table of energies, the effect of basis sets, and Cartesian coordinates for all the optimized species along modeled systems I and II.

Acknowledgments

We gratefully thank the National Natural Science Foundation of China (NNSF) (Nos. 20732003 and 20772085) and the Specialized Research Fund for the Doctoral Program of Higher Education (No. 200906101007) for financial support.

[1] a) K. A. Jørgensen, *Angew. Chem. Int. Ed.* **2000**, *39*, 3558–3588; b) K. C. Nicolaou, S. A. Snyder, T. Montagnon, G. Vassilikogiannakis, *Angew. Chem. Int. Ed.* **2002**, *41*, 1668–1698; c) E. J. Corey, *Angew. Chem. Int. Ed.* **2002**, *41*, 1650–1667; d) E. M. Stocking, R. M. Williams, *Angew. Chem. Int. Ed.* **2003**, *42*, 3078–3115.

[2] a) G. E. Keck, X. Y. Li, D. Krishnamurthy, *J. Org. Chem.* **1995**, *60*, 5998–5999; b) W. Q. Yang, D. J. Sheng, Y. L. Liu, Y. Du, X. M. Feng, *J. Org. Chem.* **2005**, *70*, 8533–8537.

[3] C. Baker-Glenn, N. Hodnett, M. Reiter, S. Ropp, R. Ancliff, V. Gouverneur, *J. Am. Chem. Soc.* **2005**, *127*, 1481–1486.

[4] B. Wang, X. Feng, Y. Huang, H. Liu, X. Cui, Y. Jiang, *J. Org. Chem.* **2002**, *67*, 2175–2182.

[5] a) M. A. McCarrick, Y. D. Wu, K. N. Houk, *J. Am. Chem. Soc.* **1992**, *114*, 1499–1500; b) D. Regas, J. M. Ruiz, M. M. Afonso, J. A. Palenzuela, *J. Org. Chem.* **2006**, *71*, 9153–9164.

[6] a) A. Zulauf, M. Mellah, R. Guillot, E. Schulz, *Eur. J. Org. Chem.* **2008**, 2118–2129; b) S. E. Schaus, J. Brånalt, E. N. Jacobsen, *J. Org. Chem.* **1998**, *63*, 403–405.

[7] H. F. Du, X. Zhang, Z. Wang, H. L. Bao, T. P. You, K. L. Ding, *Eur. J. Org. Chem.* **2008**, 2248–2254.

[8] K. B. Simonsen, N. Svenstrup, M. Roberson, K. A. Jørgensen, *Chem. Eur. J.* **2000**, *6*, 123–128.

[9] M. P. Doyle, M. Valenzuela, P. Huang, *Proc. Natl. Acad. Sci. USA* **2004**, *101*, 5391–5395.

[10] R. A. Fischer, J. Weiβ, *Angew. Chem. Int. Ed.* **1999**, *38*, 2830–2850.

[11] a) J. Lu, M. L. Hong, S. J. Ji, Y. C. Teo, T. P. Loh, *Chem. Commun.* **2005**, 4217–4218; b) Y. C. Teo, J. D. Goh, T. P. Loh, *Org. Lett.* **2005**, *7*, 2743–2745; c) T. P. Loh, G. L. Chua, *Chem. Commun.* **2006**, 2739–2749; d) P. Raghunath, M. C. Lin, *J. Phys. Chem. A* **2007**, *111*, 6481–6488.

[12] Z. P. Yu, X. H. Liu, Z. H. Dong, M. S. Xie, X. M. Feng, *Angew. Chem. Int. Ed.* **2008**, *47*, 1308–1311.

[13] a) G. Ujaque, P. S. Lee, K. N. Houk, M. F. Hentemann, S. J. Danishefsky, *Chem. Eur. J.* **2002**, *8*, 3423–3430; b) H. Audrian, J. Thorhauge, R. G. Hazell, K. A. Jørgensen, *J. Org. Chem.* **2000**, *65*, 4487–4497; c) A. Bongini, M. Panunzio, *Eur. J. Org. Chem.* **2006**, 972–977; d) S. Danishefsky, E. Larson, D. Askin, N. Kato, *J. Am. Chem. Soc.* **1985**, *107*, 1246–1255; e) D. H. Ess, G. O. Jones, K. N. Houk, *Adv. Synth. Catal.* **2006**, *348*, 2337–2361.

[14] M. A. McCarrick, Y. D. Wu, K. N. Houk, *J. Org. Chem.* **1993**, *58*, 3330–3343.

[15] M. Roberson, A. S. Jepsen, K. A. Jørgensen, *Tetrahedron* **2001**, *57*, 907–913.

[16] L. R. Domingo, J. Andres, *J. Org. Chem.* **2003**, *68*, 8662–8668.

[17] X. Zhang, H. F. Du, Z. Wang, Y. D. Wu, K. L. Ding, *J. Org. Chem.* **2006**, *71*, 2862–2869.

[18] I. Iwakura, T. Ikeno, T. Yamada, *Angew. Chem. Int. Ed.* **2005**, *44*, 2524–2527.

[19] S. Baki, J. Maddalumo, A. Derdour, P. Chaquin, *Eur. J. Org. Chem.* **2008**, 3200–3208.
[20] M. J. Frisch, G. W. Trucks, H. B. Schlegel, G. E. Scuseria, M. A. Robb, J. R. Cheeseman, J. A. Montgomery Jr., T. Vreven, K. N. Kudin, J. C. Burant, J. M. Millam, S. S. Iyengar, J. J. Tomasi, V. Barone, B. Mennucci, M. Cossi, G. Scalmani, N. Rega, G. A. Petersson, H. Nakatsuji, M. Hada, M. Ehara, K. Toyota, R. Fukuda, J. Hasegawa, M. Ishida, T. Nakajima, Y. Honda, O. Kitao, H. Nakai, M. Klene, X. Li, J. E. Knox, H. P. Hratchian, J. B. Cross, C. Adamo, J. Jaramillo, R. Gomperts, R. E. Stratmann, O. Yazyev, A. J. Austin, R. Cammi, C. Pomelli, J. W. Ochterski, P. Y. Ayala, K. Morokuma, G. A. Voth, P. Salvador, J. J. Dannenberg, V. G. Zakrzewski, S. Dapprich, A. D. Daniels, M. C. Strain, O. Farkas, D. K. Malick, A. D. Rabuck, K. Raghavachari, J. B. Foresman, J. V. Ortiz, Q. Cui, A. G. Baboul, S. Clifford, J. Cioslowski, B. B. Stefanov, G. Liu, A. Liashenko, P. Piskorz, I. Komaromi, R. L. Martin, D. J. Fox, T. Keith, M. A. Al-Laham, C. Y. Peng, A. Nanayakkara, M. Challacombe, P. M. W. Gill, B. Johnson, W. Chen, M. W. Wong, C. Gonzalez, J. A Pople, *Gaussian 03*, Reversion B.05, Gaussian, Inc., Pittsburgh, PA, **2003**.
[21] a) A. D. Becke, *J. Chem. Phys.* **1993**, *98*, 5648–5652; b) C. Lee, W. Yang, R. G. Parr, *Phys. Rev. B* **1988**, *37*, 785–789.
[22] J. P. Blaudeau, M. P. McGrath, L. A. Cirtiss, L. J. Radon, *J. Phys. Chem.* **1994**, *98*, 11623–11627.
[23] a) J. P. Blaudeau, M. P. McGrath, L. A. Cirtiss, L. Radon, *J. Chem. Phys.* **1997**, *107*, 5016–5021; b) V. A. Rassolov, J. A. Pople, M. A. Ratner, T. L. Windus, *J. Chem. Phys.* **1998**, *109*, 1223–1229; c) V. A. Rassolov, M. A. Ratner, J. A. Pople, P. C. Redfern, L. A. Curtiss, *J. Comput. Chem.* **2001**, *22*, 976–984.
[24] M. Cossi, V. Barone, B. Mennucci, J. Tomasi, *Chem. Phys. Lett.* **1998**, *286*, 253–260.
[25] a) A. E. Reed, R. B. Weinstock, F. J. Weinhold, *J. Chem. Phys.* **1985**, *83*, 735–746; b) A. E. Reed, L. A. Curtiss, F. Weinhold, *Chem. Rev.* **1988**, *88*, 899–926.
[26] a) L. R. Domingo, M. Arno, J. Andres, *J. Org. Chem.* **1999**, *64*, 5867–5875; b) L. R. Domingo, J. A. Sáez, *Org. Biomol. Chem.* **2009**, *7*, 3576–3583.
[27] a) R. G. Parr, L. v. Szentpaly, S. Liu, *J. Am. Chem. Soc.* **1999**, *121*, 1922–1924; b) L. R. Domingo, *Eur. J. Org. Chem.* **2004**, 4788–4793; c) L. R. Domingo, E. Chamorro, P. Pérez, *J. Phys. Chem. A* **2008**, *112*, 4046–4053.
[28] C. D. Anderson, T. Dudding, R. Gordillo, K. N. Houk, *Org. Lett.* **2008**, *10*, 2749–2752.

Received: February 10, 2010
Published Online: May 19, 2010

